

Naval Research Laboratory

Washington, DC 20375-5000

DTIC FILE COPY



2

NRL Memorandum Report 6213

AD-A196 743

**Numerical Simulations of the Flowfield
in Central-Dump Ramjet Combustors
II. Effects of Inlet and Combustors Acoustics**

K. KAILASANATH, J. H. GARDNER J. P. BORIS AND E. S. ORAN

Laboratory for Computational Physics and Fluid Dynamics

July 8, 1988



Approved for public release; distribution unlimited.

REPORT DOCUMENTATION PAGE				Form Approved OMB No 0704-0188	
1a REPORT SECURITY CLASSIFICATION UNCLASSIFIED			1b RESTRICTIVE MARKINGS		
2a SECURITY CLASSIFICATION AUTHORITY			3 DISTRIBUTION / AVAILABILITY OF REPORT		
2b DECLASSIFICATION / DOWNGRADING SCHEDULE			Approved for public release; distribution unlimited.		
4 PERFORMING ORGANIZATION REPORT NUMBER(S) NRL Memorandum Report 6213			5 MONITORING ORGANIZATION REPORT NUMBER(S)		
6a NAME OF PERFORMING ORGANIZATION Naval Research Laboratory		6b OFFICE SYMBOL (If applicable) Code 4410	7a NAME OF MONITORING ORGANIZATION		
6c ADDRESS (City, State, and ZIP Code) Washington, DC 20375-5000			7b ADDRESS (City, State, and ZIP Code)		
8a NAME OF FUNDING / SPONSORING ORGANIZATION Office of Naval Research		8b OFFICE SYMBOL (If applicable)	9 PROCUREMENT INSTRUMENT IDENTIFICATION NUMBER		
8c ADDRESS (City, State, and ZIP Code) Arlington, VA 22217			10 SOURCE OF FUNDING NUMBERS		
			PROGRAM ELEMENT NO ONR	PROJECT NO ONR	TASK NO
			WORK UNIT ACCESSION NO.		
11 TITLE (Include Security Classification) Numerical Simulations of the Flowfield in Central-Dump Ramjet Combustors II. Effects of Inlet and Combustor Acoustics					
12 PERSONAL AUTHOR(S) Kailasanath, K., Gardner, J.H., Boris, J.P. and Oran, E.S.					
13a TYPE OF REPORT Interim		13b TIME COVERED FROM 10/85 TO present		14 DATE OF REPORT (Year, Month, Day) 1988 July 8	
15 PAGE COUNT 40					
16 SUPPLEMENTARY NOTATION					
17 COSATI CODES			18 SUBJECT TERMS (Continue on reverse if necessary and identify by block number)		
FIELD	GROUP	SUB-GROUP	Ramjet, Turbulence, Combustion instability.		
19 ABSTRACT (Continue on reverse if necessary and identify by block number) A potentially important source of large pressure oscillations in compact ramjets is a combustion instability induced by the interaction of large-scale vortex structures with the acoustic modes of the ramjet. To study these interactions, we have performed time-dependent, compressible numerical simulations of the flow field in an idealized ramjet consisting of an axisymmetric inlet and a combustor. The simulations indicate strong coupling between the flow field and the acoustics of both the inlet and the combustor. For the cases studied, forcing at the first longitudinal acoustic mode of the combustor induces vortex-rollup near the entrance to the combustor at that frequency. A low frequency oscillation is also observed in all the simulations. Pressure and velocity fluctuations in the inlet indicate that the low frequency corresponds to a quarter-wave mode in the inlet. Changing the length of the inlet appropriately changes the observed low frequency. The merging pattern of the vortices in the combustor is significantly modified when either the acoustics of the combustor or that of the inlet is changed. These merging patterns are explained on the basis of an interaction between the vortex-rollup frequency and the acoustic modes of the inlet and combustor.					
20 DISTRIBUTION / AVAILABILITY OF ABSTRACT <input checked="" type="checkbox"/> UNCLASSIFIED/UNLIMITED <input type="checkbox"/> SAME AS RPT <input type="checkbox"/> DTIC USERS			21 ABSTRACT SECURITY CLASSIFICATION UNCLASSIFIED		
22a NAME OF RESPONSIBLE INDIVIDUAL Kazhikathra Kailasanath			22b TELEPHONE (Include Area Code) (202) 767-2402		22c OFFICE SYMBOL Code 4410

CONTENTS

1. Introduction	1
2. The Numerical Model	3
3. Acoustic-Vortex Interactions	5
4. Low-Frequency Oscillations	9
5. Acoustics and Merging Patterns	14
6. Summary and Conclusions	17
7. Acknowledgements	19
8. References	20



Accession For	
NTIS GRA&I	<input checked="" type="checkbox"/>
DTIC TAB	<input type="checkbox"/>
Unannounced	<input type="checkbox"/>
Justification	
By	
Distribution/	
Availability Codes	
Dist	Avail and/or Special
A-1	

NUMERICAL SIMULATIONS OF THE FLOWFIELD IN CENTRAL-DUMP RAMJET COMBUSTORS

II. EFFECTS OF INLET AND COMBUSTORS ACOUSTICS

1. Introduction

Solid and liquid propellant rockets and air-breathing engines, such as ramjets, have a tendency towards combustion instability. In general, strong instabilities in combustors are not desirable because they can cause excessive mechanical vibrations on the engine and other parts of the vehicle. Mild instabilities may, however, improve combustion efficiency by increasing fuel-oxidizer mixing. Therefore it is very important to understand the mechanisms leading to combustion instabilities and to learn to control them. A number of possible mechanisms, such as, vortex shedding from flameholders and steps¹⁻⁴ and acoustic response of the inlet and combustor⁵⁻⁷, have been proposed.

A characteristic feature of the geometric configuration of a ramjet is a sudden increase in area. The flow separates at this location and the separated shear layer is usually turbulent under ramjet operating conditions. Such transitional shear layers are characterized by large-scale coherent vortical structures. The interactions among these vortical structures can generate acoustic waves. Furthermore, the interactions themselves can be affected by the acoustic waves in the ramjet. The nonlinear interactions among acoustic waves, large-scale vortex structures and chemical energy release can result in destructive combustion instability.

This paper is the second in a series which presents the results of numerical simulations performed to isolate and study the interaction between acoustic waves and large-scale vortex structures in an idealized, central-dump ramjet combustor. The first report dealt primarily with tests of the model and the effects of acoustic forcing²⁰. In this report we focus on the effects of the inlet and combustor acoustics. The objective is to determine the extent to which acoustic waves influence vortex-rollup and merging patterns in the confined geometry of a combustor.

In recent years, numerical simulations have been used to study the flow field in both axisymmetric centerbody⁸ and dump combustors⁹⁻¹². In the numerical study of a dump-combustor flow field⁹, there was fair agreement between the computed quantities such as mean axial velocity profiles and experimental data. However, these computations predicted

a steady solution with a large recirculation zone. Simulations of a centerbody combustor⁸ showed an oscillating flow field with periodic vortex shedding. Neither of these simulations considered the effects of an exit nozzle or acoustic waves on the flow field in the combustor. More recent simulations have considered the effects of exit nozzles¹⁰⁻¹² and the acoustics of the inlet and combustor^{10,12}.

In earlier papers^{10,12,20}, the effects of acoustic forcing were studied by comparing calculations with and without forcing. These simulations showed that forcing at the first longitudinal acoustic mode of the combustor induces vortex-rollup near the entrance to the combustor at the forcing frequency. However, in these simulations, the frequency of the first longitudinal mode of the combustor was close to the initial vortex-rollup frequency observed in the unforced calculations. Comparisons of calculations¹² with and without forcing also showed that forcing results in enhanced mixing, in agreement with experimental observations^{13,14}. An interesting feature observed in the simulations was the presence of a low-frequency oscillation. The entire flow in the combustor was periodic at this low frequency. The frequency of this mode is measured to be nearly that of the quarter-wave mode in the inlet.

In all of our previous calculations^{10,12,20}, the flow parameters and the dimensions of the inlet and combustor were the same. This paper extends the previous work by considering the effects of systematically changing the lengths of the inlet and the combustor on the vortical flow field. Changing the lengths of the inlet and combustor, while maintaining the same inflow parameters, changes their longitudinal acoustic frequencies. This is shown to have significant effect on the vortex rollup and merging frequencies in the combustor. In particular, the effects of the low-frequency oscillation on the merging patterns and the periodicity of the flow field are discussed. The physical mechanism causing the low frequency oscillation is also clarified.

2. The Numerical Model

The numerical model used to perform the simulations solves the compressible, time-dependent, conservation equations for mass, momentum and energy in a two-dimensional axisymmetric geometry. The algorithm used for convection is Flux-Corrected Transport (FCT)¹⁵, a conservative, monotonic algorithm with fourth-order phase accuracy. FCT algorithms can be constructed as a weighted average of a low-order and a high-order finite-difference scheme. During a convective transport timestep, FCT first modifies the linear properties of the high-order algorithm by adding diffusion. This prevents dispersive ripples from arising, and it ensures that all conserved quantities remain monotonic and positive. Then FCT subtracts out the added diffusion in regions away from discontinuities. Thus it maintains a high order of accuracy while enforcing positivity and monotonicity. With various initial and boundary conditions, this algorithm has been used previously to solve a wide variety of problems in both supersonic reacting flows^{16,17} and subsonic turbulent shear flows^{10,12,18,19}.

The calculations presented below are inviscid, that is, no explicit term representing physical viscosity has been included in the model. Also, no artificial viscosity is needed to stabilize the algorithm. There is a residual numerical diffusion present which effectively mimics a viscosity term for short-wavelength modes on the order of the zone size. Unlike most numerical methods, however, the damping of the short-wavelength modes is nonlinear. Thus the effects of this residual nonlinear diffusion diminish very quickly for the long wavelength modes. This results in a high effective Reynolds number. In the problem considered in this paper, the focus is on the interaction of the acoustic modes with large-scale vortex structures, which is essentially an inviscid interaction.

The calculations reported here are essentially large-eddy simulations which model the fluid instabilities leading to a transition to turbulent flow. Although an explicit subgrid turbulence model is not included in these calculations, the nonlinear cutoff of high frequency modes by the FCT algorithm acts as a subgrid model.

A schematic of the idealized central-dump combustor used in the simulations is shown

in Fig. 1. A cylindrical jet with a prescribed mean velocity (50 m/s for the simulations described here) flows through an inlet of diameter, D into a cylindrical combustion chamber (dump combustor) of larger diameter. The dump combustor acts as an acoustic cavity and its length is varied to change the frequency of the first longitudinal mode. An annular exit nozzle at the end of the chamber is modelled to produce choked outflow.

The initial thrust of the modelling was to develop appropriate inflow and outflow boundary conditions^{10,20}. The outflow conditions force the flow to become sonic at the throat of the exit nozzle. At the solid walls the normal flux is set to zero and the pressure is extrapolated to the normal stagnation condition. At the inflow, the pressure is allowed to fluctuate, but the mass flow rate and the inflow velocity are specified. These conditions allow the acoustic waves to reflect without amplification or damping at the inflow. These inflow boundary conditions could be modified to partially damp the acoustic waves originating downstream. More detailed discussions and tests of the boundary conditions have been presented in earlier papers^{12,20}.

For the calculations presented in this paper, the computational cell spacing was held fixed in time. Fine zones were used near the entrance to the combustor (the dump plane) in both the radial and axial directions. In both directions the cell sizes gradually increased away from the dump plane. The effects of numerical resolution were checked by comparing calculations with 20×50 , 40×100 and 80×200 cells. These grids were generated by either doubling or halving the cell sizes used in the 40×100 cell calculations. The 20×50 was too coarse to resolve the vortex shedding and merging resolved by the other two grids. With the finer 80×200 grid, smaller structures and higher frequencies can be resolved than with the coarser (40×100) grid. However, it was found that the 40×100 grid was adequate to resolve the major frequencies and all the large-scale structures observed in the cold flow^{12,20}. Therefore, this grid is used in all the calculations reported here.

3. Acoustic-Vortex Interactions

The numerical simulations predict values of the density, momentum and energy for each of the computational cells as a function of time. From this information we can selectively generate the data required for various diagnostics. In the analysis presented below, we use two types of diagnostics extensively: the fourier analysis of local, time-dependent velocity and pressure fluctuations at various locations in the ramjet, and instantaneous flow visualization at selected times. Streamlines are primarily used for flow visualization and they allow us to correlate and track the coherent vortex structures and their merging patterns.

In the calculations discussed below, a portion of the rear wall of the dump combustor acts as an acoustic source, simulating a planar loudspeaker. The forcing amplitude is 0.5% of the initial chamber pressure and the frequency is that of the first longitudinal acoustic mode of the dump combustor.

Case 1: Basic Configuration — a Combustor of length 5.8 D

The physical dimensions of the inlet and combustor used in the first set of calculations are given in Fig. 1. In addition, the exit consists of an annular ring at 0.64 D (from the axis of the combustor) with an area of 7.99 cm². The mass inflow rate is 0.38 kg/s with a mean velocity of 50 m/s. The initial chamber pressure is 186 kPa. These conditions were chosen to match those in the experiments of Schadow et al.^{13,14} In this case the forcing frequency is 450 Hz. This corresponds to the first longitudinal acoustic mode of the combustor and is also in the range of the most amplified frequencies near the dump plane¹³. A calculation similar to this case has been discussed extensively in earlier papers^{12,20} and is therefore only summarized below. In the earlier simulations, the exit was at 0.69 D with an area of 8.69 cm². This resulted in a mean chamber pressure lower than the initial values and hence the acoustic frequencies were also lower.

Streamlines of the instantaneous flow field provide evidence that forcing in the range of the most amplified frequency near the dump plane produces highly periodic and coherent vortex structures. Figure 2 shows the streamlines within the dump combustor at a sequence

of times. The various frames in this figure are instantaneous "snapshots" of the flow field taken 1.093 ms apart. This corresponds to 1000 timesteps in the calculation. In each frame, the dump plane is at the left and the exit plane is at the right. The paths of the various vortices are also indicated in the figure. In the first frame (timestep 31000), there is a vortex structure near the dump plane. In the second frame (timestep 32000), this structure has grown and moved downstream. In the third frame (timestep 33000), not only has this structure moved further downstream, but a new structure has formed near the dump plane. This process continues with a new vortex structure appearing near the dump plane at intervals of 2000 timesteps. This corresponds to a frequency of 458 Hz, which is close to the forcing frequency of 450 Hz. The small discrepancy of 8 Hz is an artifact of showing the flow field snapshots at intervals of 1000 timesteps rather than 1017 timesteps.

Figure 2 also shows that the two structures, first seen near the dump plane at timesteps 31000 and 33000, have merged (paired) at about 2.4 D by timestep 37000. As this large, merged structure moves downstream, another vortex, first seen near the dump plane at timestep 35000, merges with it. This new merging occurs by timestep 43000 at about 4.8 D. The structures which appeared near the dump plane at timesteps 37000 and 39000 merge together at about 2.4 D by timestep 43000. That is, at either 2.4 D or 4.8 D, a merging is observed only at about every 6000 timesteps which corresponds to a frequency of about 150 Hz. Two successively generated vortices do not always merge with each other because new vortices appear near the dump plane every 2000 timesteps.

The time evolution of the flow field described above can be correlated with the fourier analysis of the pressure and velocity fluctuations observed at various axial locations in the combustor. The fourier analysis of the velocity fluctuations at the six axial locations, 0.1, 1.05, 2.03, 3.03, 4.07 and 5.14 D are shown in Fig. 3. All the locations are at the level of the step, a constant radial distance of 0.5 D from the axis of the combustor. At 0.1 D, the dominant frequency is 450 Hz. This is at least partly due to the velocity fluctuations associated with the forcing frequency of 450 Hz. Some of it may also be due

to velocity fluctuations associated with the vortex-rollup seen in Fig. 2. The amplitude at 450 Hz increases significantly as one moves downstream to 1.05 D. This corresponds to the passage frequency of the vortices first seen near the dump plane. There is also some amplitude at 150 Hz. The amplitude at 150 Hz increases further by 2.03 D and that at 450 Hz decreases. This is because of the vortex mergings which have begun to occur. By 3.03 D, the vortex merging is complete and the 450 Hz is no longer significant. This is consistent with the flow field visualization in Fig. 2 which shows vortex mergings near 2.4 D at a frequency of about 150 Hz.

At 2.03 and 3.03 D, there is a new feature in the spectrum: there is significant amplitude at 300 Hz. As discussed earlier, two successively generated vortices do not always merge with each other at 2.4 D. Therefore, between 2.03 and 3.03 D, both vortex mergings are seen as well as a smaller vortex passing by that eventually merges with the larger one. This smaller vortex passes by once between successive mergings. Because successive mergings occur with a frequency of 150 Hz, there are velocity fluctuations at the higher frequency of 300 Hz. At 4.07 D, the dominant frequency is 150 Hz corresponding to the passage of the vortex that was formed by merging between 2.03 and 3.03 D. At 5.14 D, the dominant frequency is 150 Hz because of the mergings that take place near 4.8 D at that frequency. Furthermore, there is no longer a significant amplitude at 300 Hz because only one type of large merged vortex passes by 5.14 D.

An interesting feature in the frequency spectrum at 5.14 D is that the amplitude at 75 Hz is comparable to that at 150 Hz. This frequency (75 Hz) is also seen weakly at some of the other locations. More careful examination of the flow field in Fig. 2 shows that although the flow field undergoes a complete cycle at a frequency of 150 Hz (6000 timesteps), there are small variations between two successive cycles. Thus the flow field is really quasi-periodic at 150 Hz and is more nearly periodic at 75 Hz. Further analysis is needed to determine whether the flow field is ever really periodic or whether there are always some differences at even lower frequencies.

The fourier analysis of the pressure fluctuations at the same six axial locations is

shown in Fig. 4. It corroborate the observations based on the velocity fluctuations and the flow field visualization. The acoustic-forcing frequency of 450 Hz is also seen to some extent at all locations. The pressure-fluctuation spectrum at 5.14 D shows many more frequencies than the velocity-fluctuation spectrum. The difference between the amplitudes at 450 Hz in the two spectrums is noteworthy. There are significant fluctuations at 450 Hz in the pressure, but not in the velocity. This is because 5.14 D is close to the end wall of the combustor which is a pressure anti-node for the first longitudinal mode. There are also some structures at both 4.07 D and 5.14 D at a high frequency of about 3160 Hz. These may be due to transverse acoustic modes of the chamber. These modes are expected to be more prominent near the exit because the flow turning to exit through the nozzle causes more transverse flow in this region. These modes were also seen in earlier numerical simulations^{10,12}, in which they were also prominent in the early stages of the development of flow.

4. Low-frequency Oscillations

Figure 2 shows that the entire flow undergoes a complete cycle in approximately 6000 timesteps. For example, at timesteps 33,000 and 39,000, a large-scale structure has partially exited through the nozzle. At these times, there are also similar flow structures of about the same sizes at about the same positions in the chamber. This similarity exists between any two frames which are 6000 timesteps apart. The frequency corresponding to this repetition is about 150 Hz. This frequency is one third of the forcing frequency or the first vortex merging frequency near the dump plane. It is also essentially the same as that observed in earlier numerical simulations^{10,12}, in which a low frequency of about 144 Hz was seen in calculations without and with forcing at 446 Hz.

The low frequency oscillation can be generated by a number of mechanisms, such as the interactions between the vortices and the wall of the combustor or the nozzle and interactions between different acoustic modes of the ramjet and the flow field. Some of these mechanisms have been discussed in earlier papers and it was found that the observed low frequency was close to the frequency of the quarter-wave mode in the inlet¹². Therefore, a mechanism associated with the acoustics of the inlet is examined below in some detail.

The inlet is essentially a long pipe with flow coming in from one end and flowing out into the combustor at the other end. The inflow boundary conditions specified in the numerical model allow complete reflection of the pressure waves that reach the upstream end of the inlet. If the downstream end of the inlet behaves like an open end, the dominant acoustic mode of the inlet would be the quarter-wave mode. Because the length of the inlet is 8.8 D, the frequency of this mode for the physical conditions in the simulation discussed above is about 148 Hz, which is close to the observed frequency of 150 Hz.

The fourier analyses of pressure fluctuations at various locations in the inlet are shown in Fig. 5. The dominant frequency near the upstream end of the inlet (-8.13 D) is indeed 150 Hz, but there are also fluctuations at 450 Hz. Closer to the combustor, the amplitude of the 150 Hz mode decreases and that of the 450 Hz mode increases. If the downstream end of the inlet behaves like an open end, the amplitude at 150 Hz should decrease as

one moves towards it and reach zero at the dump plane. This is indeed the trend. There are fluctuations at 450 Hz because there are pressure fluctuations at this frequency near the combustor-step and this signal propagates both upstream and downstream. The mode shape in the inlet, corresponding to 450 Hz is complex because this frequency does not match the frequency of any simple acoustic modes of the inlet.

Figure 5 confirms that 150 Hz corresponds to the quarter-wave mode in the inlet. However, it also shows that the amplitude of the pressure fluctuations at the inlet-combustor junction is minimal at this low frequency. Therefore, the pressure fluctuations are probably not causing the observed low-frequency mergings in the combustor.

The time history of the velocity fluctuations at a location close to the inlet-combustor junction is shown in Fig. 6a. This shows that the velocity fluctuates with a period of about 2.2 ms which corresponds to a frequency of about 450 Hz. However, the magnitude of the fluctuations is significantly smaller every third cycle which corresponds to a frequency of 150 Hz. The effect of this change in the magnitude of the velocity fluctuations is to change the strength of the vortices shed from the combustor-step. It was shown earlier that the vortex-shedding (or rollup) frequency was 450 Hz. Therefore, every third vortex has a slightly different strength from the other two. The time history of vorticity fluctuations near the inlet-combustor junction shown in Fig. 6b corroborates this observation. The effect of having every third vortex with a very different strength from the others is to create two merging locations within the combustor.

The calculation discussed so far has shown that the vortex shedding or rollup frequency matches the first longitudinal mode of the combustor and that the vortex-merging pattern is determined by the interaction between this frequency and the frequency of the quarter-wave mode in the inlet. The generality of this observation needs to be investigated. This has been done by independently changing the lengths of the inlet and the combustor.

Case 2: Shorter Inlet

In order to confirm that the acoustics of the inlet determines the low-frequency and merging pattern in the combustor, the length of the inlet was decreased to 7.2 D. The

fourier analysis of the pressure fluctuations at a series of axial locations in the inlet is shown in Fig. 7. The low-frequency oscillation has appropriately shifted to 174 Hz, which is the frequency of the quarter-wave mode for this inlet length.

Figure 7 shows that in addition to the low-frequency fluctuations at 174 Hz, velocity fluctuations are also occurring at 450 Hz at some locations in the inlet. This implies that the vortex shedding frequency has not changed from 450 Hz. If the interaction between the quarter-wave mode in the inlet and the vortex-shedding frequency is what determines the merging pattern, then it should be quite different for this case.

The instantaneous flow field in the combustor at a sequence of distinct time is shown in Fig. 8. The time interval between successive frames is again 1.093 ms, which corresponds to 1000 timesteps in the simulations. At first glance, the flow field is very different from that corresponding to the Case 1. However, new vortical structures near the dump plane are observed at timesteps 30000, 32000, 34000, 36000, etc., that is, at the same frequency of 450 Hz as in the previous case. As expected, the vortex roll-up frequency has not changed by changing the length of the inlet.

The merging pattern for Case 2 seen in Fig. 8 is rather complicated, showing some features seen in Case 1 and others which are different. As in Case 1, two vortices merge by step 33000 at about 3.3 D, and before the merged vortex exits the combustor, another vortex merges with it by step 38000. The next two vortices appearing near the dump plane (at timesteps 34000 and 36000) merge by step 39000 at about 3.3 D. This merged vortex exits the combustor without any further mergings. The next two vortices merge with a third vortex. Therefore, the vortex-merging pattern in the combustor is an alternating pattern of three and then two vortices merging together. The entire flow field repeats itself nearly every 10000–11000 timesteps. During this cycle, there are two vortex mergings at 3.3 D occurring approximately every 5250 Hz, but only one at 5.1 D. The frequencies of velocity fluctuations at various locations within the combustor are shown in Fig. 9.

The spectra in the first two frames of Fig. 9 are qualitatively very similar to those in Fig. 3. This is because the initial vortex rollup process is essentially the same in the

two cases. In both cases, the vortex rollup frequency is 450 Hz and matches the first longitudinal acoustic mode frequency of the combustor. At 2.03 D and 3.03 D, there are fluctuations at two low frequencies, 174 Hz and 276 Hz. These two frequencies are analogous to the frequencies 150 Hz and 300 Hz observed in Case 1. The 174 Hz fluctuation is related to the vortex mergings occurring in the middle of the combustor at this frequency and the 276 Hz fluctuation occurs because every fifth vortex passes by these locations without merging. At locations further downstream, the dominant frequency is 174 Hz, but there are also fluctuations at about 90 Hz. This is the frequency with which every fifth vortex merges with the larger vortex composed of every third and fourth vortex shed from the combustor-step.

The two cases discussed above show that the acoustics of the inlet play an important role in determining the flow field in the combustor. In both cases, the low frequency matches the frequency of the quarter-wave mode of the inlet. Below, the effect of the changing the length and therefore the acoustics of the combustor is studied.

Case 3: Longer Combustor

In this case, the length of the combustor was increased to 8.6 D and all other dimensions were the same as those in Case 1. The flow velocity as well as the grid resolution in the radial direction are the same as in Cases 1 and 2, implying that the natural instability frequency of the shear layer is the same as in the previous cases. The forcing frequency was decreased to 300 Hz to match the frequency of the first longitudinal mode of this longer combustor.

The instantaneous flow field within the combustor at a sequence of timesteps is shown in Fig. 10. A new large-scale structure appears near the dump plane at intervals of about three thousand timesteps, that is, at timesteps 40000, 43000, 46000, 49000 and 52000. This corresponds to a frequency of about 300 Hz, which is the same as the forcing frequency. The first conclusion from changing the length of the combustor is that the vortex roll-up frequency near the dump plane changes to match the first longitudinal mode frequency of the combustor. In order to confirm this observation, a similar calculation but without any

acoustic forcing was also performed. That simulation also showed the same vortex rollup frequency, implying that indeed the first longitudinal mode of the combustor, atleast over a significant range, is the determining factor.

Fig. 10 shows that two successively generated vortices merge with each other at about 3.5 D. No further mergings occur as the vortices convect downstream and exit through the nozzle. This is in contrast to Case 1, in which a further merging with a single vortex occurred before the pair could exit. The frequency corresponding to the vortex mergings is about 150 Hz as it occurs at approximately every 6000 timesteps. The lowest dominant frequency observed in Case 1 was also 150 Hz. *The low frequency does not change when the length of the combustor is increased.* Instead, the merging pattern has changed to accomodate the same low frequency of 150 Hz. This reinforces the conclusion that the low frequency is determined by the quarter-wave mode of the inlet and the merging pattern is determined by the interaction between the acoustics of the combustor and the inlet.

The frequency spectrum of the velocity fluctuations at a series of six axial locations in the shear layer is shown in Fig. 10. The two dominant frequencies are 150 and 300 Hz. As expected, the amplitude at 300 Hz reaches a maximum at about 1.56 D before any mergings occur within the combustor. The amplitude at 150 Hz reaches a maximum between 3.01 and 4.5 D because a vortex merging occurs between these two locations.

5. Acoustics and Merging Patterns

The three cases discussed above indicate that the shear layer at the inlet-combustor junction responds to the acoustics of both the inlet and the combustor. The relation between the low frequency and the merging patterns has many features similar to the experimental observations of Ho and Huang²¹ on vortex mergings in a mixing layer. They observed different merging patterns depending on the relation between the forcing frequency and the frequency at which vortices initially form in the mixing layer. For example, when the forcing frequency was one-third of the frequency at which vortices initially form, first two vortices merged and then this large vortex merged with a third vortex. This pattern is similar to that observed in Case 1. The similarity between the observations of the experiments and the calculations suggests that the low frequency observed in the simulations acts as an additional forcing or modulating frequency on the shear layer near the dump plane. Though the exact details of this interaction are not yet clear, the effect of the low frequency perturbation is to change the strength of the successive vortices periodically as discussed earlier.

Extending the analogy between the experiments and the calculations to Case 3, only one merging is expected because the low frequency is one-half of the initial vortex-rollup frequency of 300 Hz. This is the merging pattern observed in Fig. 10. Therefore, the average number of vortices merging together in one cycle of the periodic flow field observed in the simulations is given by

$$N = \frac{f_r}{f_l}, \quad (1)$$

where f_r is the initial vortex-rollup frequency and f_l is the low frequency. Knowing these two frequencies, the merging pattern in the combustor can be predicted using the above formula.

In Case 2, the low frequency is not a sub-multiple of the frequency of the first longitudinal mode of the combustor. Using Eq.(1) to predict the merging pattern for this case gives a value of 2.6 for N . Because the number of vortices merging together have to

be an integral number, two vortices merge together in one cycle followed by three vortices merging in the next cycle, giving an average of 2.5 for the number of vortices merging per cycle. Therefore, Eq. (1) holds for all the cases simulated, even when the low frequency is not a sub-multiple of the frequency of the first longitudinal mode of the combustor. However in such cases, the flow field is not quite as periodic as in cases when the vortex roll-up frequency is an integral multiple of the low frequency.

Case 4: An Intermediate Length Combustor

In order to test the generality of the above conclusions, another simulation was performed in which the lengths of the inlet and combustor were interchanged from those used in Case 2. In Case 4, the length of the combustor is 7.2 D and the length of the inlet is 8.6 D. The forcing frequency was 358 Hz and the other parameters were kept the same as in the above calculations. Based on the previous results, the vortex-rollup frequency should be 358 Hz, the low frequency should be about 150 Hz, and there should be three vortices merging in one cycle and two merging in the next.

The instantaneous flow field in the combustor at a sequence of timesteps is shown in Fig 12. The time interval between successive frames is again 1.093 ms, which corresponds to 1000 timesteps in the simulations. There are new vortical structures near the dump plane at timesteps 41000, 44000, 46000, 49000, 51000, etc., corresponding to an average frequency of about 2500 timesteps or 366 Hz. It is not exactly 358 Hz as expected because the flow field contours are shown only every 1000 timesteps, that is, at finite intervals of 915 Hz. However, the fourier analyses of the pressure and velocity fluctuations show that the dominant frequency is indeed 358 Hz.

The merging pattern in Fig. 12 is similar to that of Case 2, and shows features seen in both Cases 1 and 3. The two vortices near the dump plane at timesteps 40000 and 41000 merge by step 47000 at about 3.6 D, and exit the combustor by step 50000. There is no further merging after the merging at 3.6 D. This merging pattern is similar to that seen in Case 3. The next two vortices appearing near the dump plane (at timesteps 44000 and 46000) merge by step 52000 at about 3.6 D. However, before this large vortex exits

the combustor, another vortex merges with it by step 60000 at about 6.7 D. This merging pattern is similar to that of Case 1. Therefore, the flow field in this combustor exhibits features of both the combustors considered earlier.

The frequency of merging at 3.6 D is about 5000 timesteps or about 180 Hz. The frequency of merging at 6.7 D is nearly 13000 timesteps or about 70 Hz. The entire flow field shown in Fig. 12 repeats approximately every 13000 timesteps. During this period two vortices exit the combustor. That is, the frequency with which a vortex exits the combustor is approximately 6500 timesteps or 140 Hz. which is very nearly the same as the low frequency observed in two previous cases.

6. Summary and Conclusions

The numerical simulations indicate that the acoustics of the ramjet, both the inlet and the combustor, play a dominant role in determining the flow field. A number of simulations, in which the lengths of the inlet and combustor were varied, were used to isolate the roles of the acoustics of the inlet and the combustor. In all the cases studied, a low frequency oscillation is observed. Pressure and velocity fluctuations in the inlet indicate that the acoustics of the inlet is the origin of this low frequency. Changing the length of the inlet changes the observed low frequency appropriately. The vortex-merging pattern in the combustor is also significantly different when the inlet length is changed.

For the cases studied, forcing at the the first longitudinal acoustic mode of the combustor induces vortex rollup near the entrance to the combustor at that frequency. That is, the shear layer responds to a range of forcing frequencies. In the cases discussed in detail here, the forcing frequencies have been 450, 300 and 358 Hz. All of these frequencies are probably close to the most amplified frequency of the unforced shear layer corresponding to these cases. Therefore, forcing at these frequencies induces vortex rollup near the entrance to the combustor at that frequency. Numerical simulations in which the shear layer thickness is varied, are currently being performed, to study further the interaction between the natural instability frequencies of the shear layer and the longitudinal modes of the combustor.

In the three cases where the length of the combustor is changed, the lowest dominant frequency does not change significantly from 150 Hz. However, the merging patterns of the vortices in the combustor change significantly. In Case 1, the forcing frequency was 450 Hz. Here two vortices merge with each other, but before the large vortex exits the combustor, a third vortex merges with it. This results in mergings at two locations within the combustor and at each location the merging frequency is 150 Hz. The frequency with which the merged vortices exit the combustor is also 150 Hz. In Case 3 with a longer combustor, the forcing frequency was 300 Hz. In this case there is only one merging location within the combustor. Mergings occur at a frequency of 150 Hz and the merged

vortices exit at this frequency. In Case 4, the length of the combustor was between those of the above cases and the forcing frequency was 358 Hz. The flow field is complicated and shows features of both of the above cases. There are two merging locations where mergings occur at different frequencies. The average frequency with which the merged vortices exit the combustor is approximately 143 Hz. These simulations indicate that the merging pattern is determined by the interaction between the low frequency and the vortex-rollup frequency.

The relation between the low frequency and the merging patterns has also been studied. The various cases simulated suggest that the low frequency in the inlet acts as an additional perturbation on the shear layer at the inlet-combustor junction. The merging pattern in the combustor is determined by the interaction between the vortex roll-up frequency and the low frequency.

7. Acknowledgements

This work was sponsored by the Office of Naval Research and the Naval Air Systems Command. The authors would like to thank Drs. Klaus Schadow, Fernando Grinstein, and Joseph Baum for their many helpful discussions and suggestions. The support and encouragement from Dale Hutchins at NAVAIR, Jack Hansen at ONR and Douglas Davis at AFWAL is greatly acknowledged.

8. References

1. Keller, J.O., Vaneveld, "Mechanism of Instabilities in Turbulent Combustion Leading to Flashback," AIAA Paper No. 81-0107, presented at the AIAA 19th Aerospace Sciences Meeting, Jan. 1981.
2. Abouseif, G.E., Keklak, J.A., and Toong, T.Y., "Ramjet Rumble: The Low-Frequency Instability Mechanism in Coaxial Dump Combustors," *Combust. Sci. Tech.*, Vol. 36, 1984, pp. 83-108.
3. Dunlap, R. and Brown, R.S., "Exploratory Experiments on Acoustic Oscillations Driven by Periodic Vortex Shedding," *AIAA Journal*, Vol. 19, March 1981, pp. 408-409.
4. Flandro, G.A., "Vortex Driving Mechanism in Oscillatory Rocket Flows," *J. Prop. Power.*, Vol. 2, 1986, pp. 206-214.
5. Sajben, M., Bogar, T.J., and Kroutil, J.C., "Forced Oscillation Experiments in Super Critical Diffuser Flows," *AIAA Journal*, Vol. 22, April 1984, pp. 465-474.
6. Culick, F.E.C. and Rogers, T., "The Response of Normal Shocks in Diffusers," *AIAA Journal*, Vol. 21, Oct. 1983, pp. 1382-1390.
7. "ONR/AFOSR Workshop on Mechanisms of Instability in Liquid-Fueled Ramjets," CPIA publication 375, Apr. 1983.
8. Scott, J.N., and Hankey, W.L., "Numerical Simulation of Cold Flow in an Axisymmetric Centerbody Combustor," *AIAA Journal*, Vol. 23, May 1985, pp. 641-649.
9. Drummond, J.P., "Numerical Study of a Ramjet Dump Combustor Flowfield," *AIAA Journal*, Vol. 23, Apr. 1985, pp. 604-611.
10. Kailasanath, K., Gardner, J.H., Boris, J.P. and Oran, E.S., "Acoustic-Vortex Interactions in an Idealized Ramjet Combustor," *Proceedings of the 22nd JANNAF Combustion Meeting, Pasadena, CA*, CPIA publication 432, Vol. 1, Oct. 1985, pp. 341-350.

11. Jou, W.H. and Menon. S., "Large Eddy Simulations of Flow in a Ramjet Combustor," *Proceedings of the 22nd JANNAF Combustion Meeting, Pasadena, CA*. CPIA publication 432, Vol. 1, Oct. 1985, pp. 331-339.
12. Kailasanath, K., Gardner, J., Boris, J. and Oran, E., "Interactions Between Acoustics and Vortex Structures in a Central Dump Combustor." AIAA paper 86-1609. an extended version appears in *J. Prop. Power*, Vol. 3, Nov-Dec. 1987. pp. 525-533.
13. Schadow, K.C., Wilson, K.J., Crump, J.E., Foster, J.B. and Gutmark, E.. "Interaction Between Acoustics and Subsonic Ducted Flow with Dump." AIAA paper No. 84-0530. presented at the AIAA 22nd Aerospace Sciences Meeting, Jan. 1984.
14. Schadow, K.C., Wilson, K.J. and Gutmark, E., "Characterization of Large-scale Structures in a Forced Ducted Flow with Dump," AIAA paper No. 85-0080. presented at the AIAA 23rd Aerospace Sciences Meeting, Jan. 1985.
15. Boris, J.P. and Book, D.L., "Solution of Continuity Equations by the Method of Flux-Corrected Transport," *Methods of Computational Physics*. Academic Press. New York, 1976, Vol. 16. Chap. 11, pp. 85-129.
16. Oran, E.S., Young, T.R. and Boris, J.P., "Application of Time- Dependent Numerical Methods to the Description of Reactive Shocks," *Seventeenth Symposium (International) on Combustion*. The Combustion Institute, Pittsburgh. 1979. pp. 43-54.
17. Kailasanath, K., Oran, E.S., Boris, J.P. and Young, T.R.. "A Computational Method for Determining Detonation Cell Size," AIAA paper No. 85-0236. presented at the AIAA 23rd Aerospace Sciences Meeting, Jan. 1985.
18. Boris, J.P., Oran, E.S., Gardner, J.H., Grinstein, F.F., and Oswald, C.E. "Direct Simulations of Spatially Evolving Compressible Turbulence- Techniques and Results." *Ninth International Conference on Numerical Methods in Fluid Dynamics*. pp. 98-102. Springer-Verlag, 1985.
19. Grinstein, F.F., Oran, E.S. and Boris, J.P., "Direct Simulation of Asymmetric Mixing in Planar Shear Flows," *J. Fluid Mech.*, Vol. 165, 1986, pp. 201-220.

20. Kailasanath, K., Gardner, J.H., Boris, J.P. and Oran, E.S.. "Numerical Simulations of the Flowfield in a Central-Dump Ramjet Combustor—I. Tests of the Model and Effects of Forcing," NRL Memorandum Report 5832, Naval Research Laboratory, Washington, D.C., 1986.
21. Ho, C.M., and Huang, L.S., "Subharmonics and Vortex Merging in Mixing Layers." *J. Fluid Mech.*, Vol. 119, 1982, pp. 443-473.

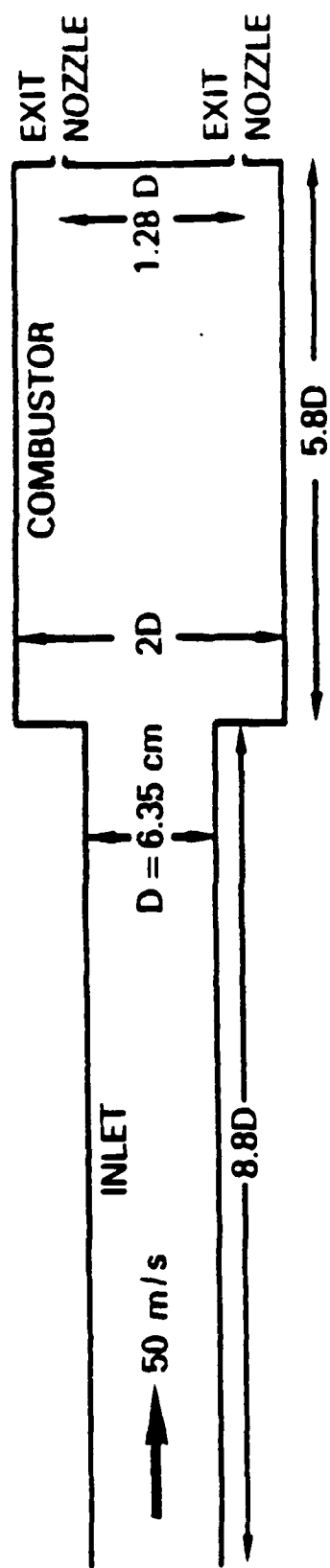


Figure 1. Basic configuration of the idealized axisymmetric ramjet combustor.

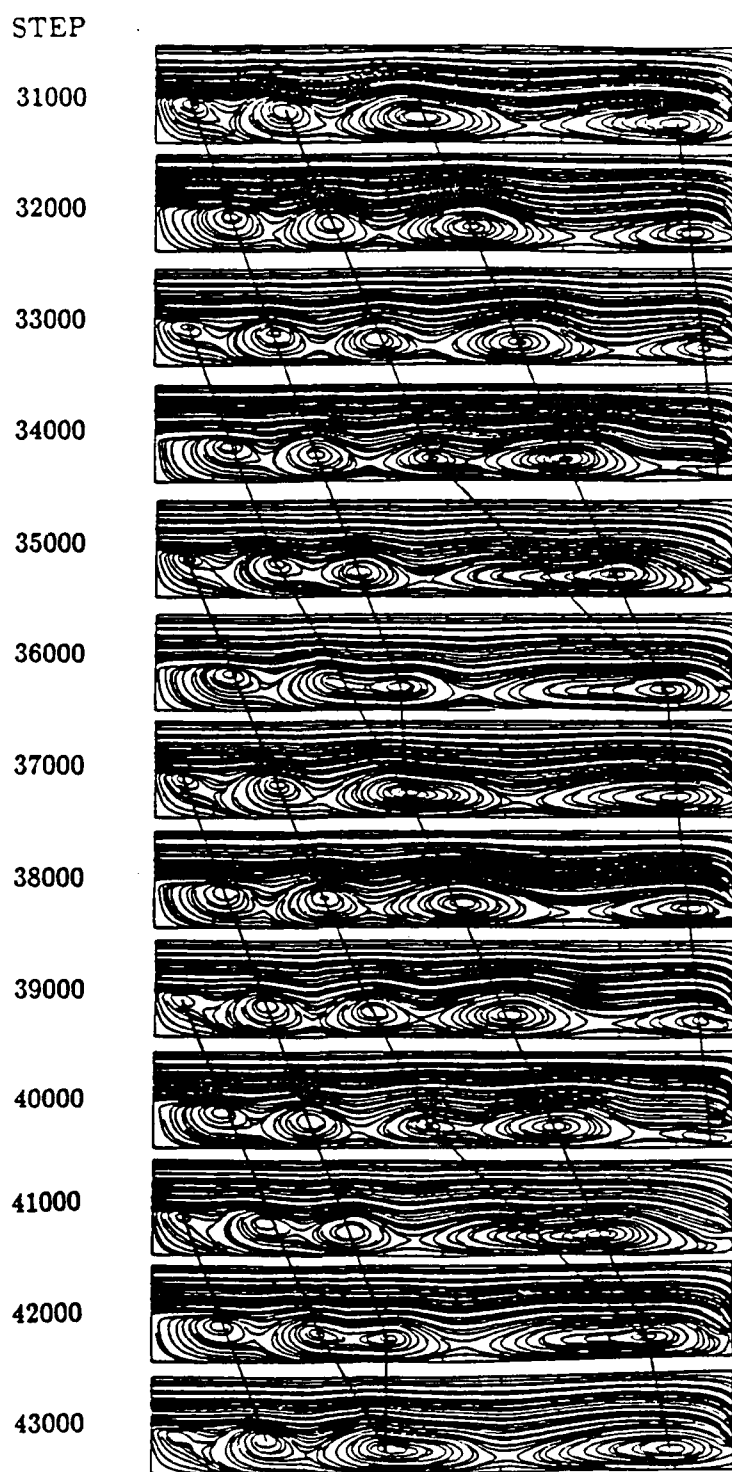


Figure 2. Streamlines showing the instantaneous flow field at a sequence of timesteps for Case 1. The time interval between any two successive frames is 1.093 ms.

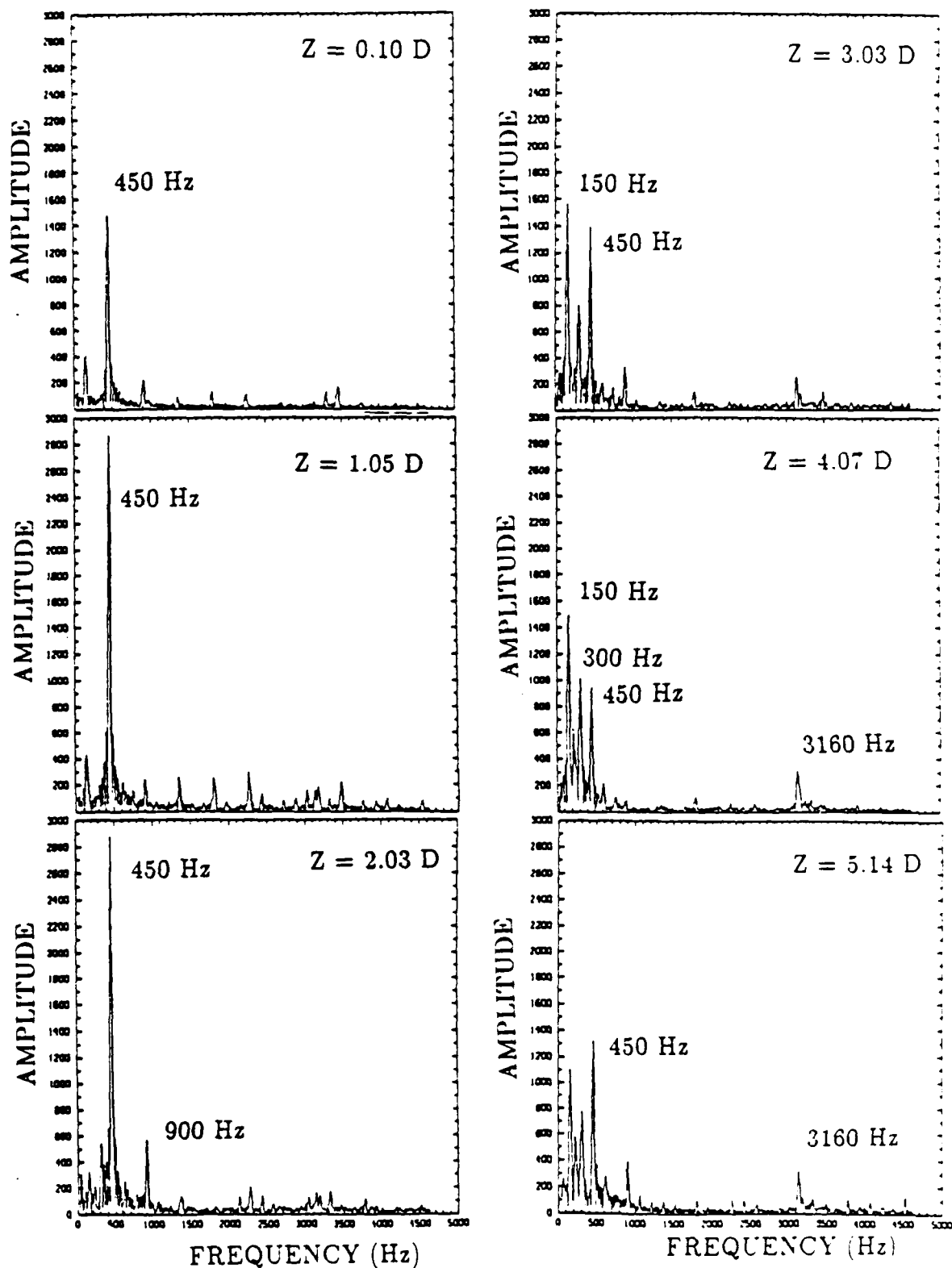


Figure 3. Frequency spectra of velocity fluctuations in the shear layer at a number of axial locations for Case 1.

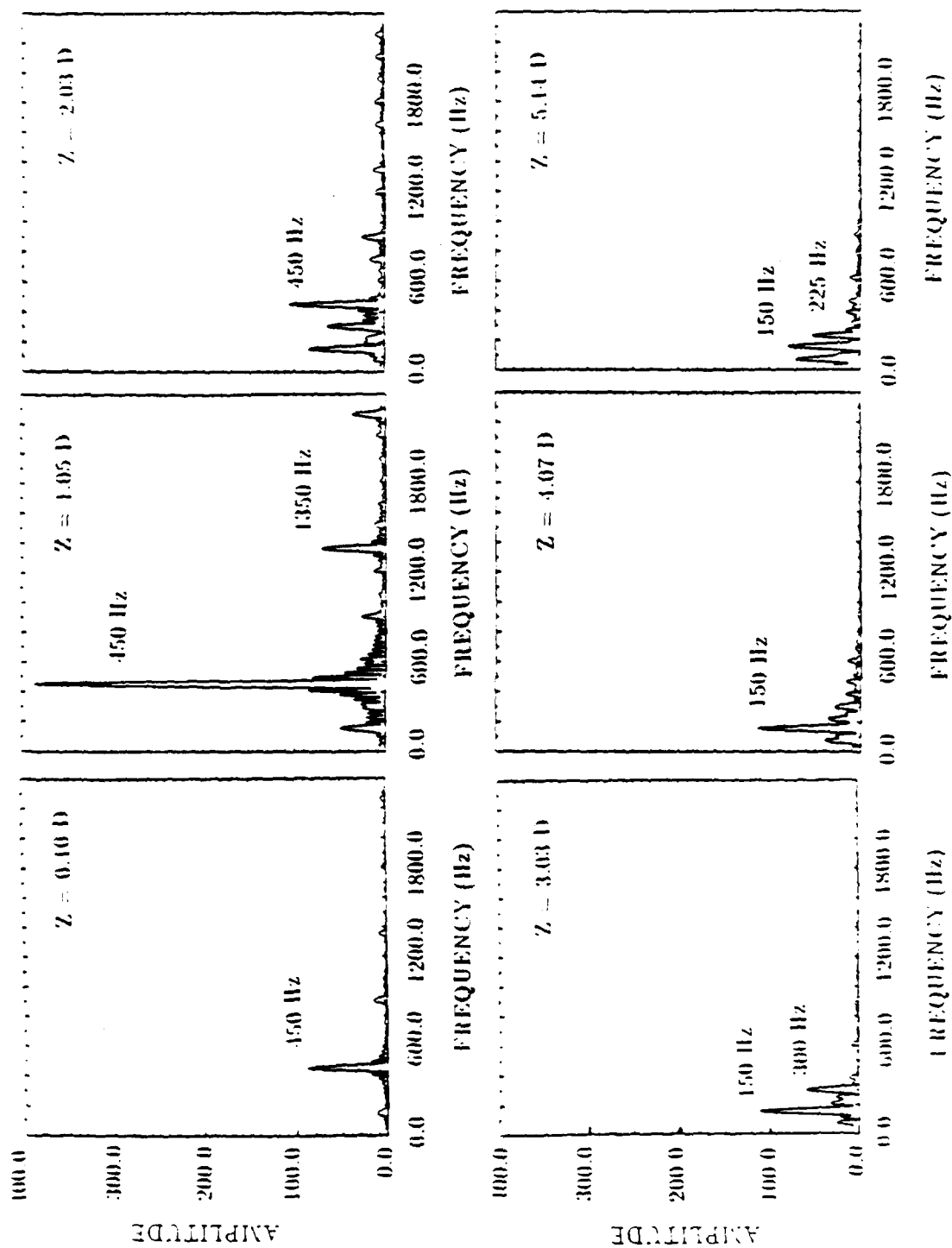


Figure 4. The frequency spectrum of pressure fluctuations in the shear layer at the same axial locations as in Figure 3 for Case 1.

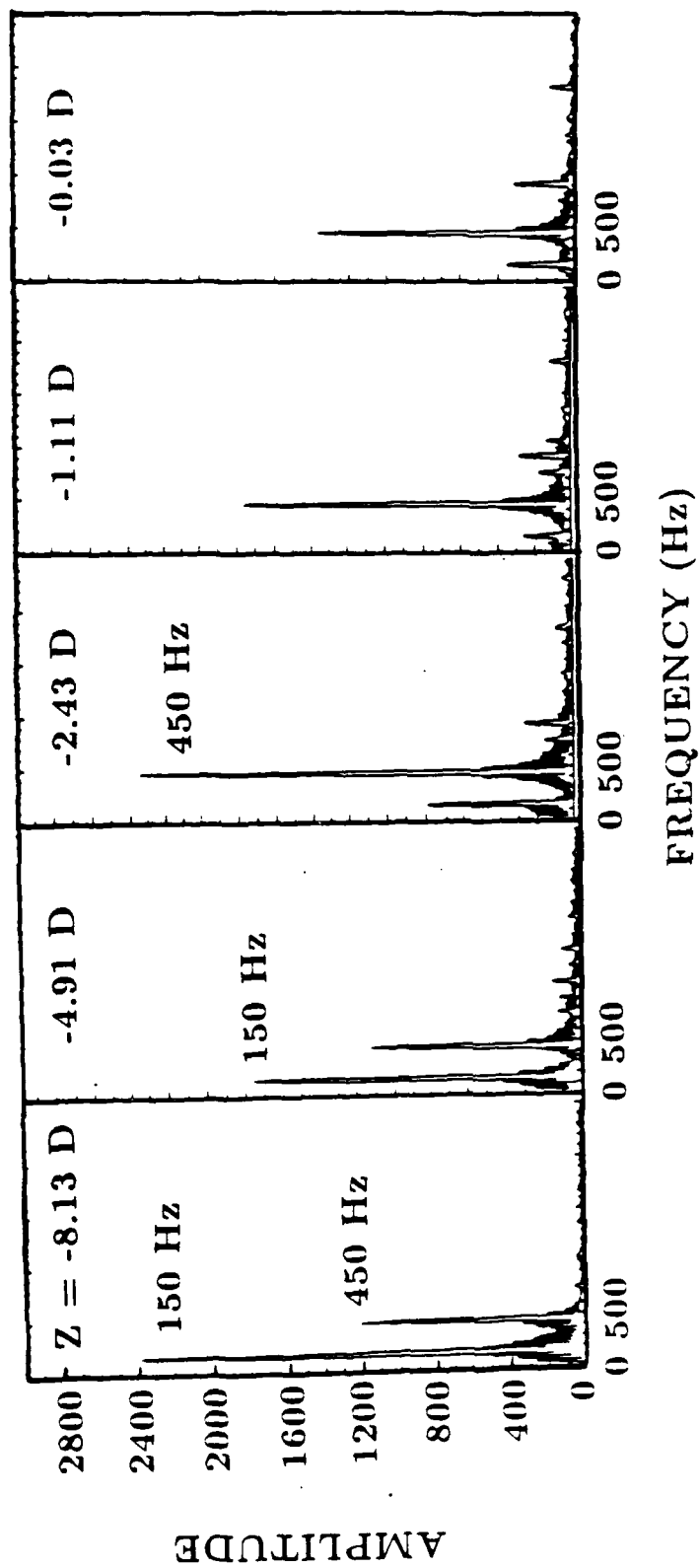


Figure 5. Frequency spectra of pressure fluctuations at five axial locations in the inlet for Case 1.

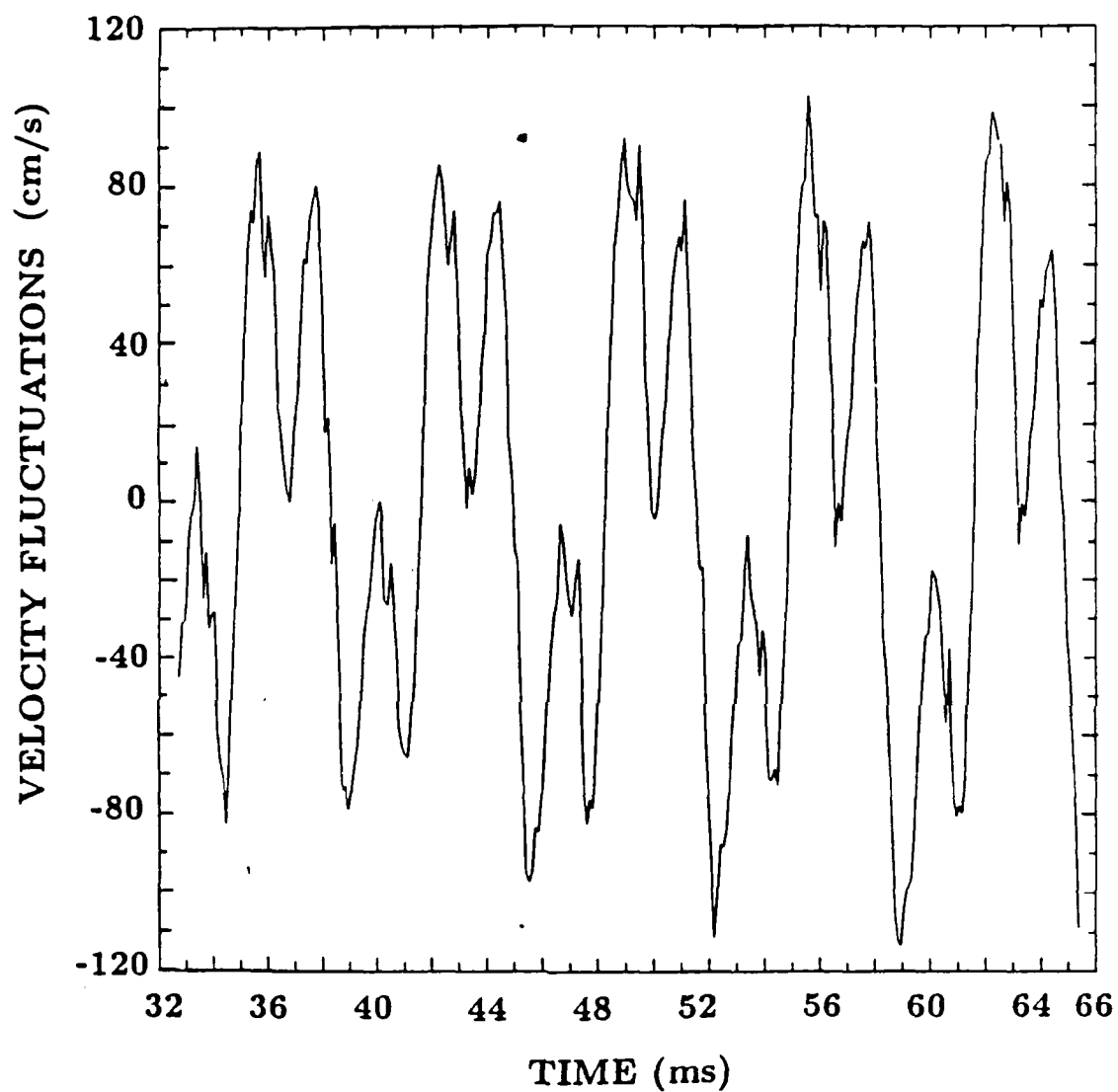


Figure 6a. Time history of velocity fluctuations near the inlet-combustor junction for Case 1. The location is $-0.03 D$.

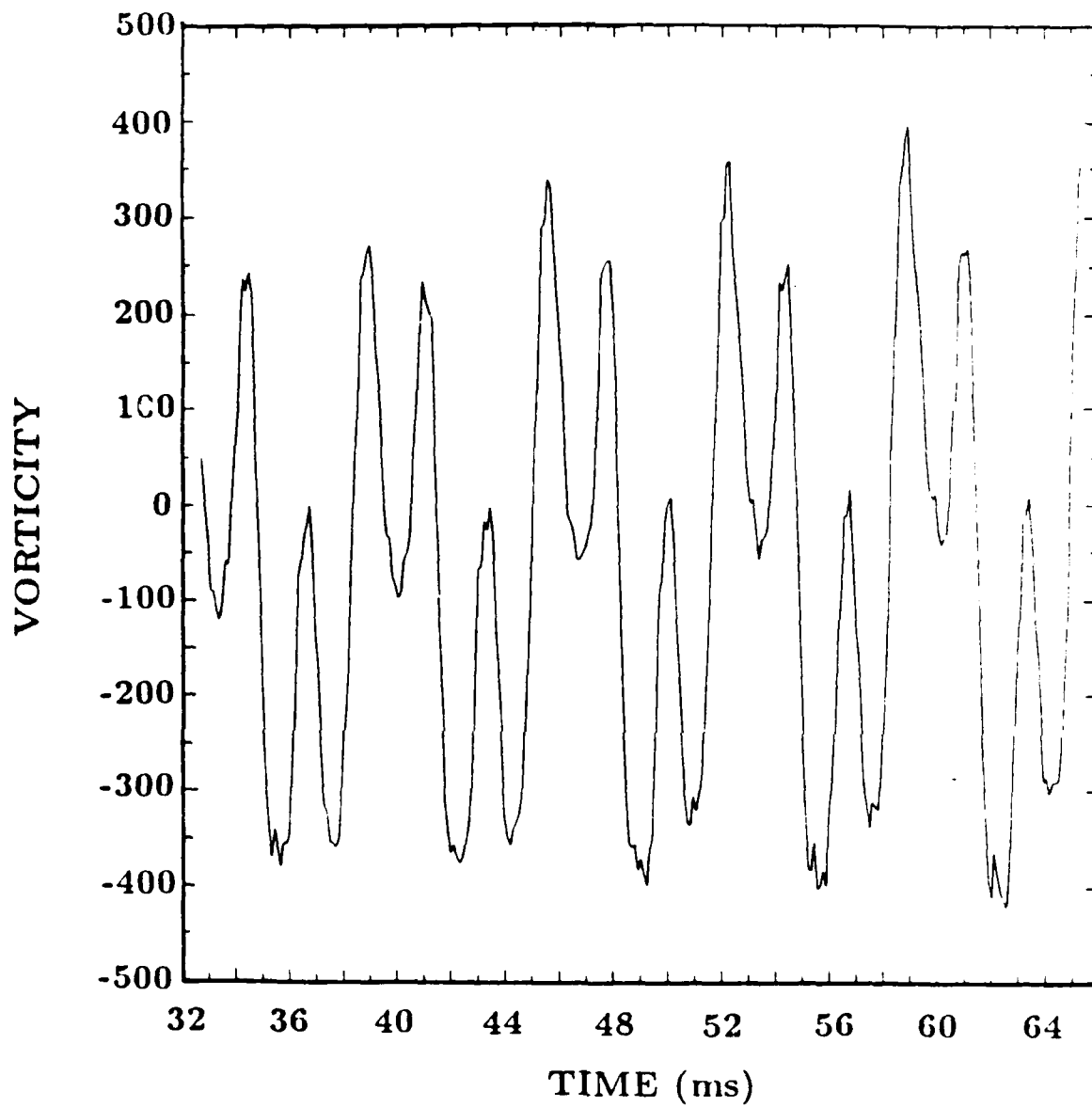


Figure 6b. Time history of Vorticity fluctuations corresponding to Fig. 6a.

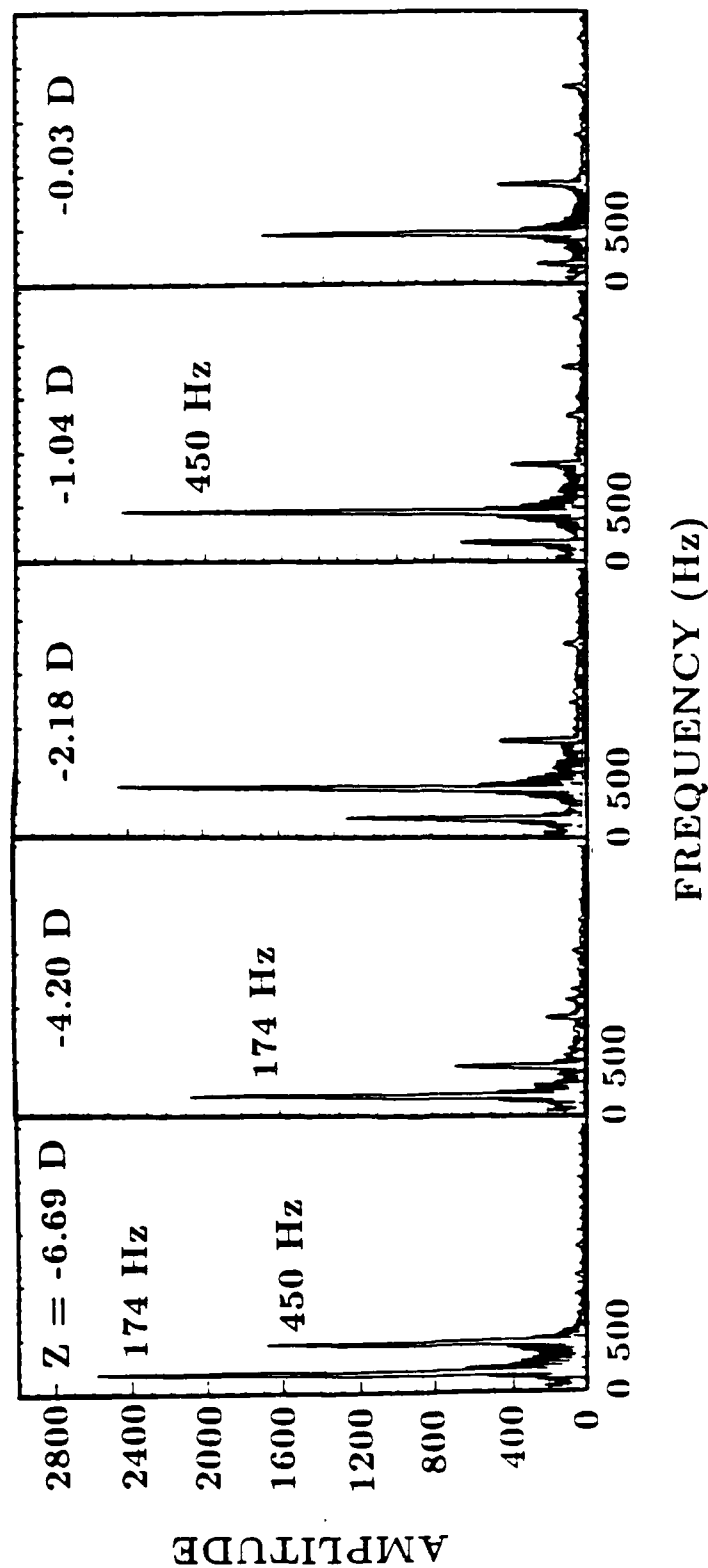


Figure 7. Frequency spectra of pressure fluctuations at five axial locations in the inlet for Case 2.

TIMESTEP

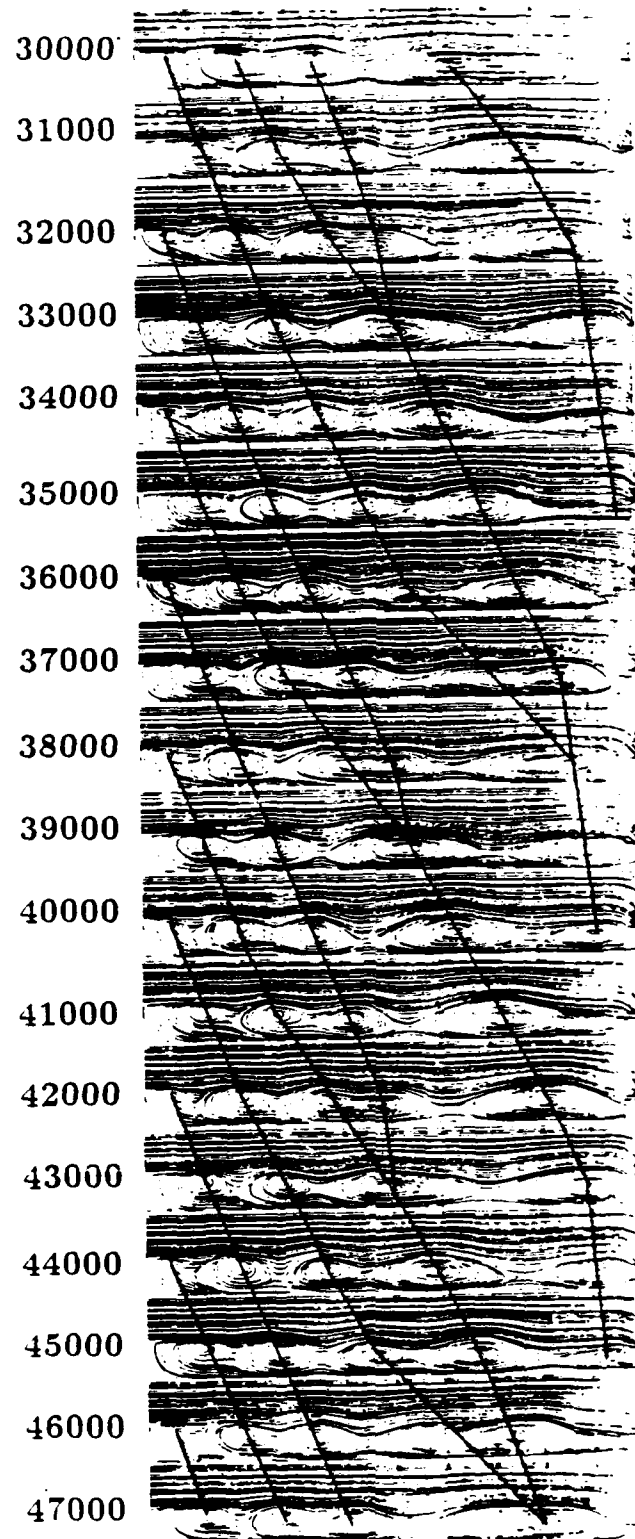


Figure 8. Streamlines showing the instantaneous flow field at a sequence of timesteps for Case 2. The length of the inlet is 7.2 D.

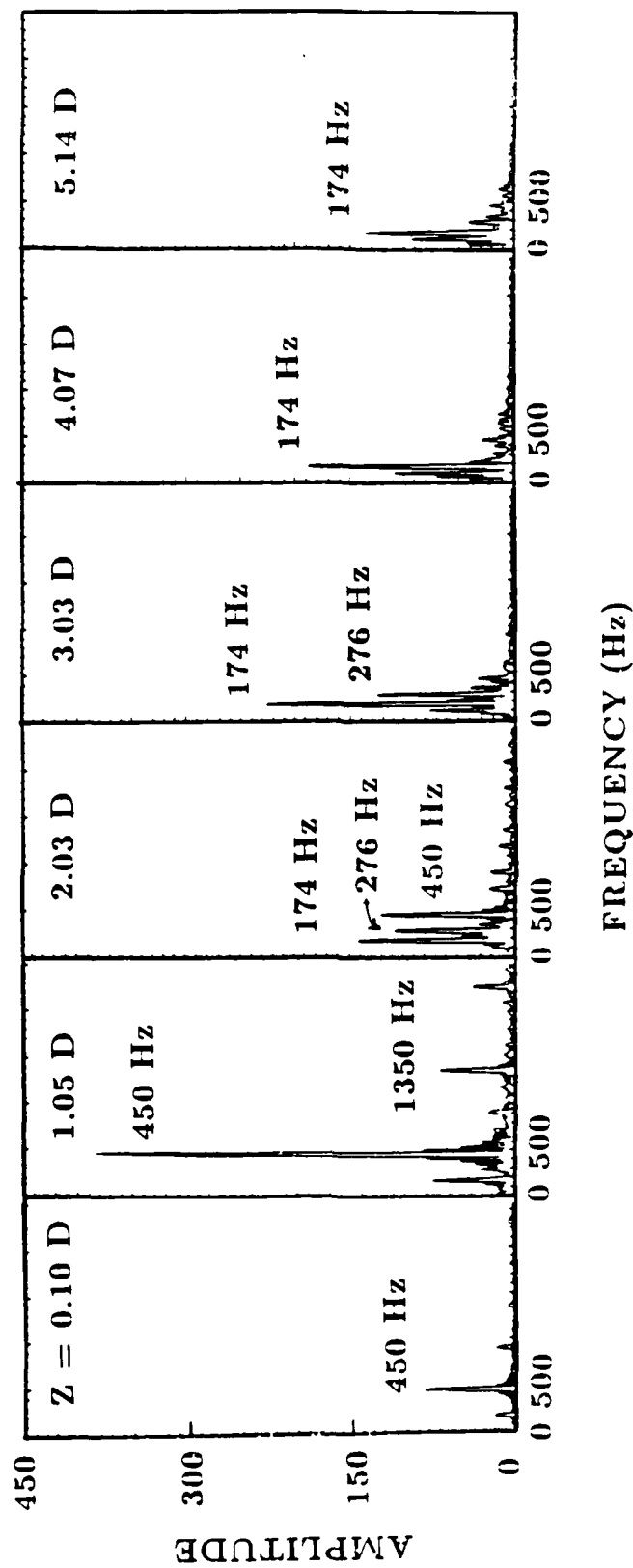


Figure 9. The frequency spectrum of velocity fluctuations in the shear layer at a number of axial locations for Case 2.

TIMESTEP

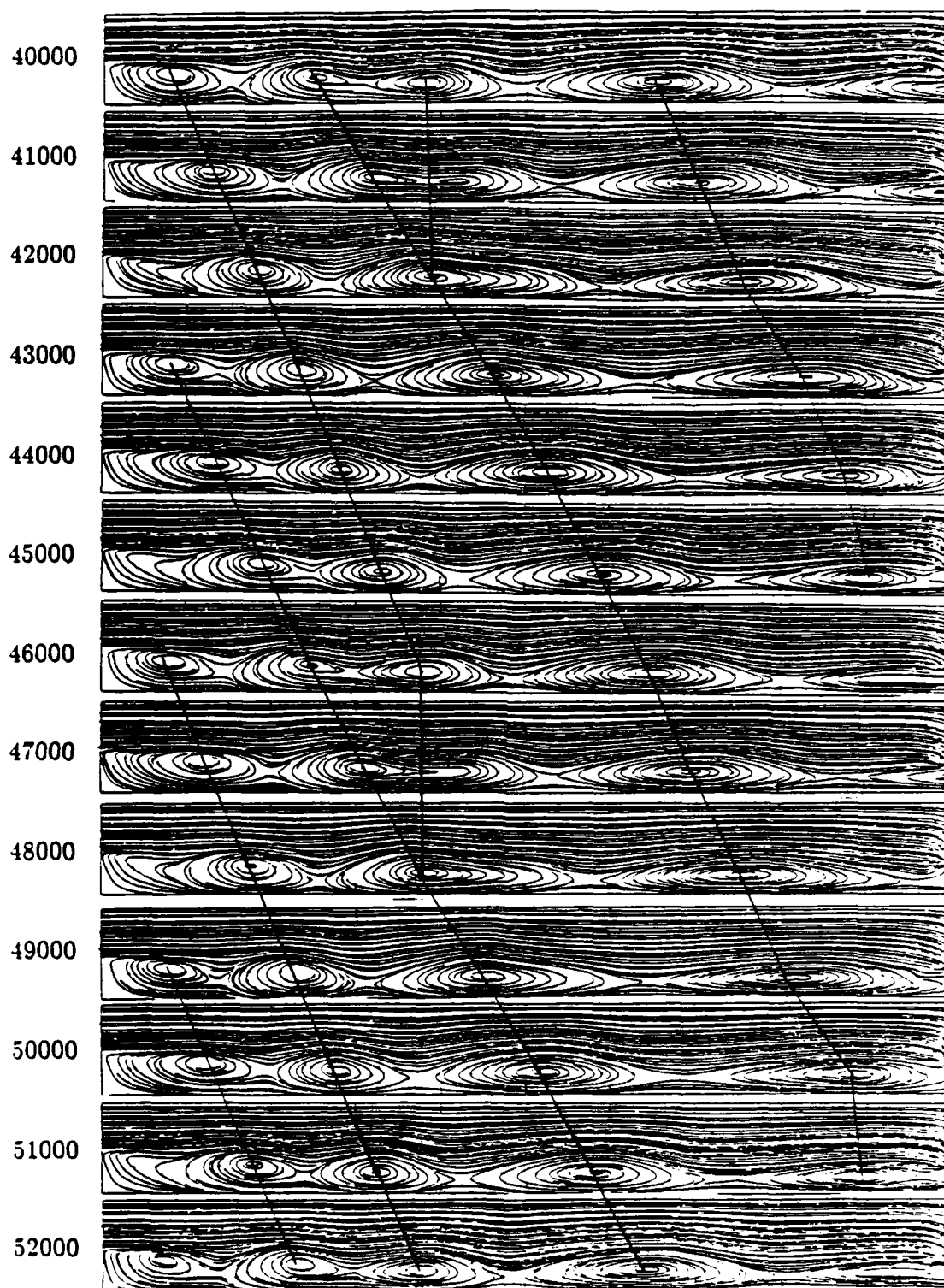


Figure 10. Streamlines showing the instantaneous flow field at a sequence of timesteps for Case 3. The length of the combustor is 8.6 D.

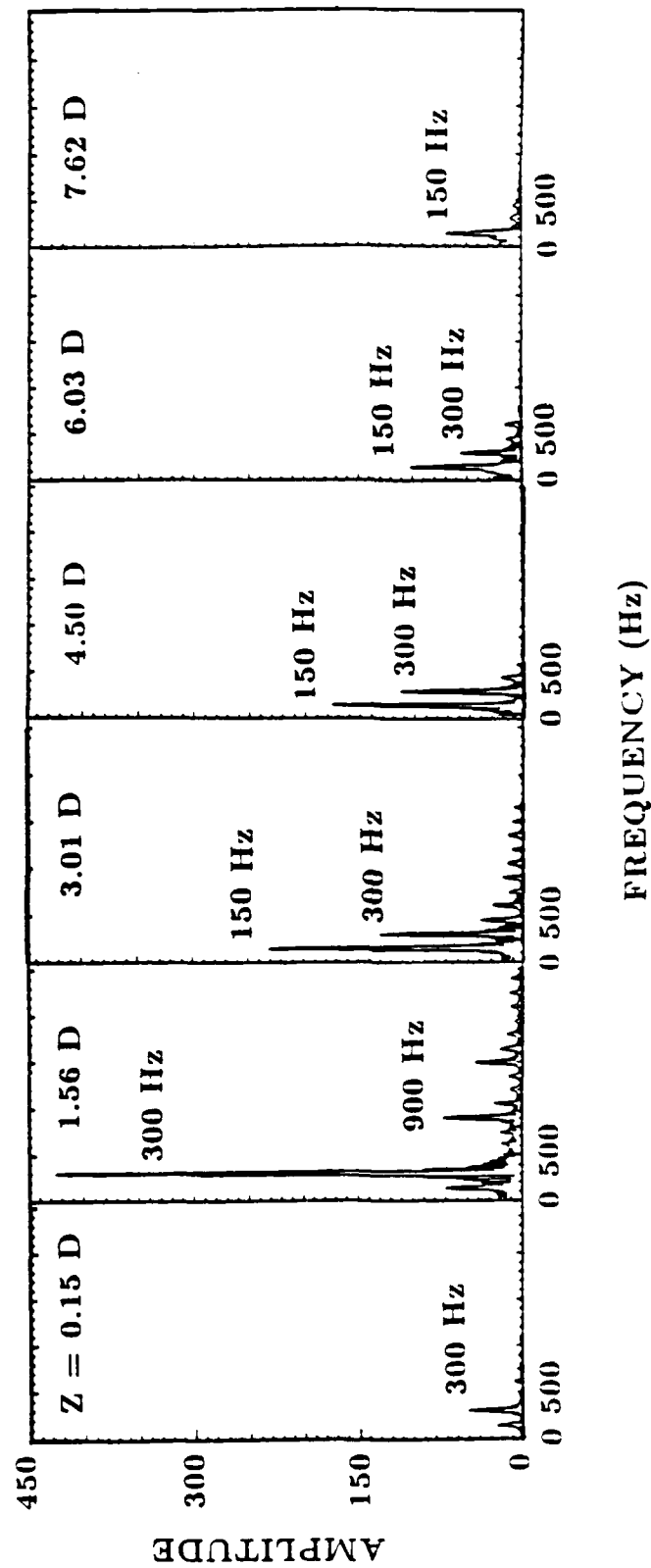


Figure 11. The frequency spectrum of velocity fluctuations in the shear layer at a number of axial locations for Case 3.

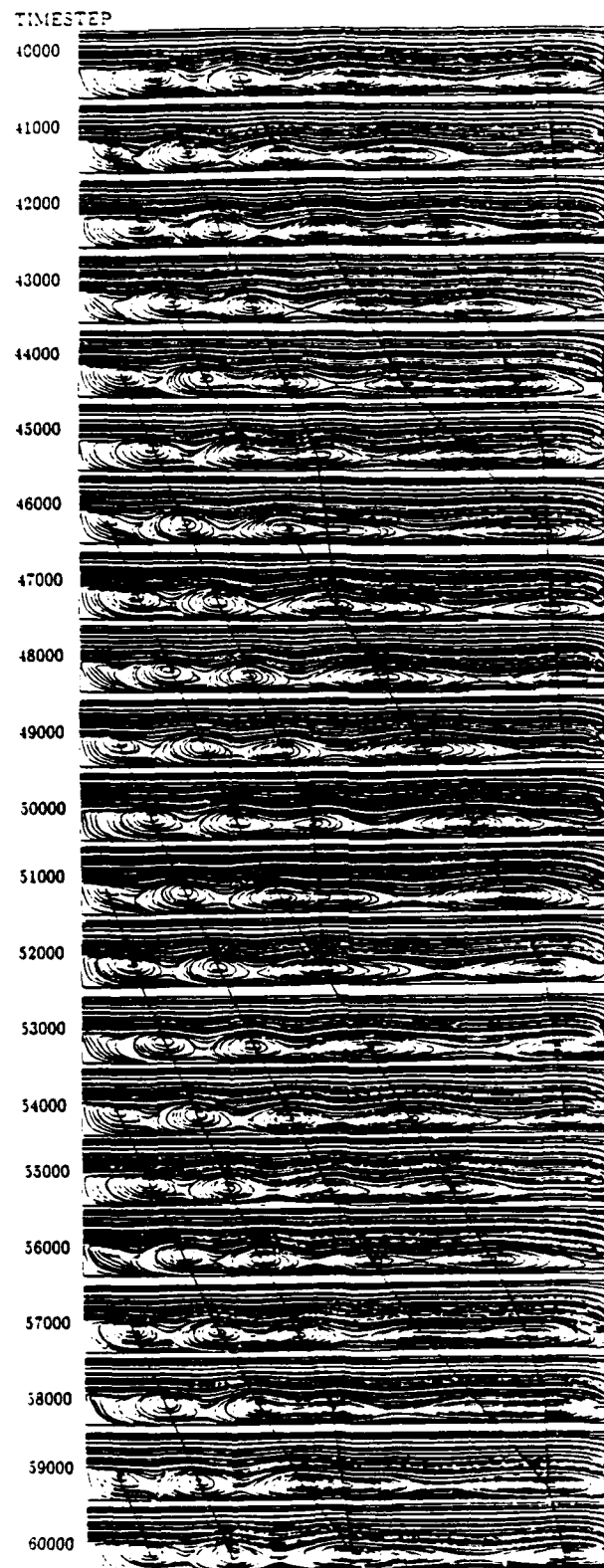


Figure 12. Streamlines showing the instantaneous flow field at a sequence of timesteps for Case 4. The length of the combustor is 7.2 D.

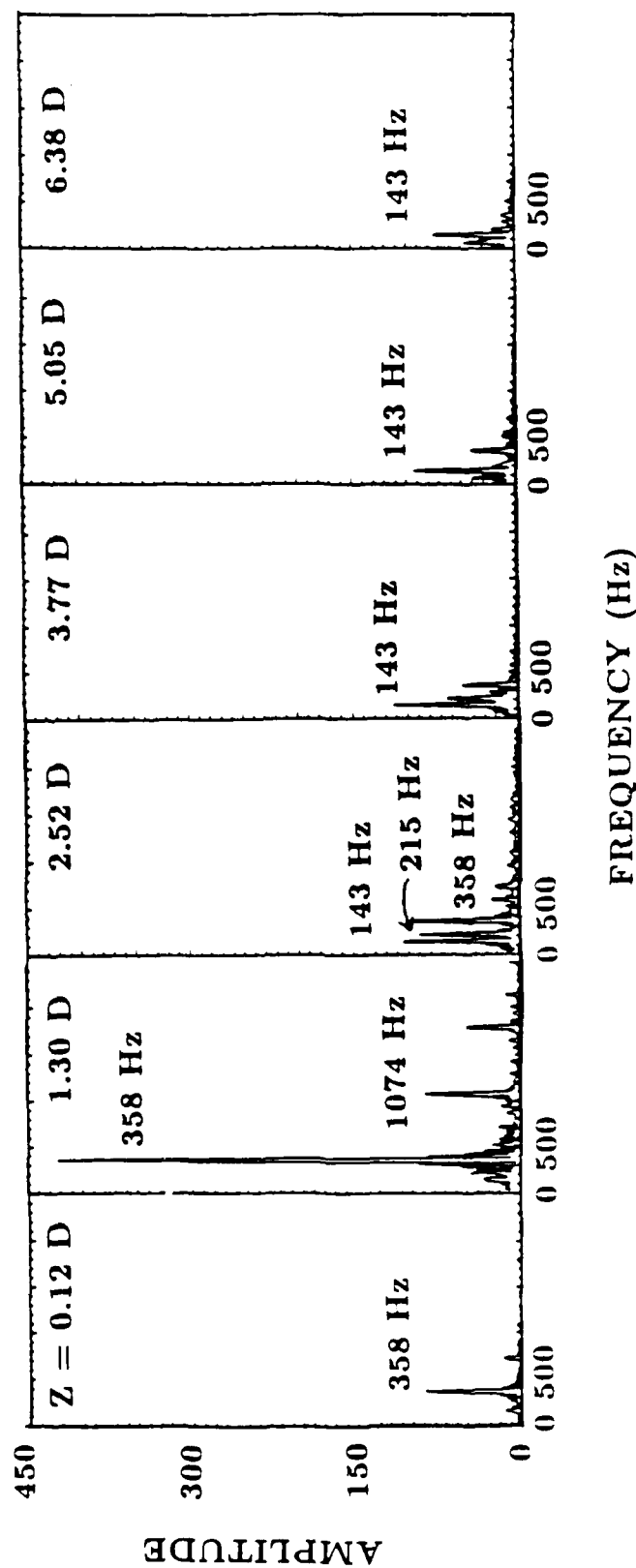


Figure 13. The frequency spectrum of velocity fluctuations in the shear layer at a number of axial locations for Case 4.